

DOI: 10.1002/cvde.200706657

Full Paper

Molecular Dynamics Simulations of the Sticking and Etch Behavior of Various Growth Species of (Ultra)Nanocrystalline Diamond Films**

By Maxie Eckert, Erik Neyts, and Annemie Bogaerts*

The reaction behavior of species that may affect the growth of ultrananocrystalline and nanocrystalline diamond ((U)NCD) films is investigated by means of molecular dynamics simulations. Impacts of CH_x ($x = 0 - 4$), C_2H_x ($x = 0 - 6$), C_3H_x ($x = 0 - 2$), C_4H_x ($x = 0 - 2$), H, and H_2 on clean and hydrogenated diamond $(100)2 \times 1$ and $(111)1 \times 1$ surfaces at two different substrate temperatures are simulated. We find that the different bonding structures of the two surfaces cause different temperature effects on the sticking efficiency. These results predict a temperature-dependent ratio of diamond (100) and (111) growth. Furthermore, predictions of which are the most important hydrocarbon species for (U)NCD growth are made.

Keywords: molecular dynamics simulations, nanocrystalline diamond, sticking and etch coefficient, ultrananocrystalline diamond

1. Introduction

Ultrananocrystalline diamond (UNCD) and nanocrystalline diamond (NCD) thin films have recently received a lot of attention due to their unique combination of physical and chemical properties, such as chemical inertness,^[1] high thermal conductivity,^[2] high hardness,^[3] high surface smoothness,^[4,5] good biocompatibility,^[6] and electrical conductivity.^[7]

UNCD films consist of fine diamond grains with diameter between 2 and 5 nm.^[8] UNCD can be grown from hydrogen poor plasmas (97% Ar/2% H_2 /1% CH_4) and at substrate temperatures (T_{sub}) as low as 700 K.^[9] NCD films have grain size diameters between 50 and 100 nm,^[8] and, in contrast to UNCD, the grain size increases as the film thickness increases.^[10] NCD films are grown under conventional diamond plasma-enhanced (PE) CVD conditions (99% H_2 /1% CH_4 , $T_{\text{sub}} \geq 1000$ K).^[9]

The physical properties of these thin films are primarily determined by the size of the diamond grains.^[1,2,11] An improved understanding of the various phenomena underlying the growth of UNCD and NCD will facilitate their

utilization in various tribological, biological, and electronic applications.^[8,12]

In the past, experimental and theoretical work has been carried out to unravel the growth mechanisms of UNCD and NCD.^[9,13,14] In particular, correlations between the composition of the plasma close to the surface and the resulting film properties were considered.^[15,16] As some hydrocarbon species (e.g. C_2H) cannot be detected by spectroscopic means under standard plasma growth conditions,^[9] computer simulations become an invaluable tool to investigate the reaction behavior of these species on an atomic scale.

In order to gain more insight into which hydrocarbon species are important for the film growth of UNCD and NCD, a series of classical molecular dynamics (MD) simulations were performed to calculate the sticking and etch coefficients of various hydrocarbon species. MD simulations allow the observation of the evolution of a system on the atomic scale, and the study of phenomena that are dynamic in nature, e.g., diamond growth by CVD.

In this study, we focus on the reaction behavior of species that may contribute to the growth of UNCD and NCD under typical conditions applied for the microwave plasma-assisted (MW) CVD of UNCD and NCD. Using MWCVD, high growth rates of the thin films can be reached and, in contrast to hot filament (HF) CVD, no filament is involved, which makes MWCVD systems inherently cleaner than HFCVD systems.^[17] Therefore, MWCVD has become the deposition system of choice for most applications of UNCD and NCD, in particular for electronic applications.^[17]

In Section 2, a description of the simulation model and computational details will be given. In Section 3, the sticking and etch behavior of the species will be presented and

[*] Prof. A. Bogaerts, M. Eckert, Dr. E. Neyts
Research group PLASMANT, Department of Chemistry,
University of Antwerp, Universiteitsplein 1, 2610 Antwerp (Belgium)
E-mail: annemie.bogaerts@ua.ac.be

[**] M. Eckert is indebted to the Institute for the Promotion of Innovation by Science and Technology in Flanders (IWT-Flanders) for financial support. E. Neyts acknowledges financial support from the Fund for Scientific Research-Flanders (FWO). The Prime Minister's Office through IUAP-VI, the Fund for Scientific Research-Flanders (FWO) and the calculation support of the core facility CALCUA, provided by the University of Antwerp, are gratefully acknowledged.

discussed. Furthermore, implications for experiments are discussed. Finally, the conclusion will be given.

2. Computational Details

In MD simulations, the time evolution of a set of interacting atoms is followed by integrating the equations of motion of the atoms. Therefore, the trajectory of every atom is followed deterministically. Since the atoms of the considered system interact with each other, the motion of the atoms results from interatomic forces. The forces acting on the atoms are calculated as the negative of the analytical derivative of the chosen interatomic potential.

The model used for this study is based on MD code that was originally developed by Tanaka et al.^[18] The interatomic potential used for this study is the well-known Brenner potential for hydrocarbons.^[19] Earlier investigations by Dyson and Smith showed that the Brenner potential, in contrast to other empirical potential functions, successfully describes the structure of diamond surfaces in agreement with quantum mechanical calculations.^[20]

In the Brenner potential, the binding energy is written as a sum over bond energies between couples of atoms. The bond energy is determined by repulsive and attractive components, which are functions of the scalar separation between the two considered atoms. The many-body chemistry is modeled by the so-called “bond order” function, which affects the value of the bond energy between the considered couple of atoms. Furthermore, the bond order function contains a correction function that accounts for the different chemistry of hydrogen and carbon.

In order to limit the potential range to first neighbors only, a cutoff function is introduced. The value of the cutoff function equals 1 for interatomic distances smaller than the inner cutoff radius (i.e., 1.7 and 1.3 Å for C–C and C–H interactions, respectively). Since the values of the repulsive and attractive components are multiplied by the cutoff function value, the attractive and repulsive components are not affected by the cutoff function for interatomic distances smaller than the inner cutoff radius. For interatomic distances greater than the outer cutoff radius (i.e., 2.0 and 1.8 Å for C–C and C–H interactions, respectively), the cutoff function value equals 0. Therefore, interactions between two atoms with interatomic distances greater than the outer cutoff radius are not taken into account for the calculation of the binding energy. Between the inner and outer cutoff radii, the cutoff function value decays smoothly from 1 to 0.

The cutoff function is used to define the bonding connectivity between atoms of the system. The number of, e.g., hydrogen atoms bonded to a given carbon atom is calculated as the sum of cutoff function values resulting from the scalar distances between the considered carbon atom and the hydrogen atoms of the system. Hence, the hybridization of each atom of the system can be identified, since it is associated with their coordination. The integration scheme used is the velocity Verlet scheme.^[21]

In order to gain more insight into which species are important for the film growth of UNCD and NCD, we focus on the reaction behavior of CH_x ($x=0-4$), C_2H_x ($x=0-6$), C_3H_x ($x=0-2$), C_4H_x ($x=0-2$), H and H_2 . These species are considered to be present close to the substrate under typical conditions applied for the MWCVD of UNCD and NCD.^[9,14] To calculate the sticking and etch coefficients of the species, impacts on clean and hydrogenated diamond (100) and diamond (111) surfaces are simulated. The diamond (100) and (111) surfaces are the two most important surfaces for diamond.^[22]

During CVD growth, the diamond surface is hydrogen-terminated by exposure to atomic hydrogen.^[17] Sticking of hydrocarbon particles to the surface can only take place at rare reactive sites (dangling bonds) that are created by hydrogen abstraction by impacting hydrogen atoms or hydrocarbon radicals (“etching”).^[17] Therefore, the configuration of the carbon atoms at the surface is very likely to correspond to the reconstruction geometry of the hydrogen-terminated surface. As a model of the reactive sites of the growing diamond surface, we constructed clean diamond (100) 2×1 and (111) 1×1 surfaces according to the geometry of the hydrogen-terminated diamond surfaces.^[23,24] In Figure 1, schematic pictures of the diamond (100) 2×1 and (111) 1×1 surfaces can be found.

The clean diamond (100) and (111) substrates contain 900 and 768 atoms, respectively. The hydrogenated diamond (100) and (111) surface contain, in addition, 50 and 64 hydrogen atoms, respectively. The lower two atomic layers (100 and 128 atoms for diamond (100) and (111), respectively) are kept static to anchor the simulation cell, preventing its translation due to momentum transfer from impacting particles.

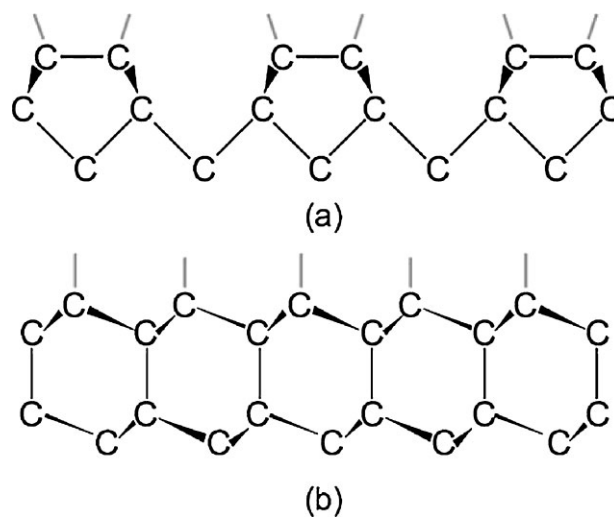


Fig. 1. Schematic side view of the a) three topmost layers of carbon atoms of the diamond (100) 2×1 surface, and b) four topmost layers of carbon atoms of the diamond (111) 1×1 surface. In both figures, the gray lines represent the dangling bonds and C–H bonds of the clean and hydrogen-terminated surface, respectively. For clarity, not all C–C bonds of the carbon atoms are shown. Every carbon atom of the topmost layer is bonded to three other carbon atoms; the other carbon atoms are four coordinated.

As UNCD can be grown at lower temperatures than NCD (see above), the sticking coefficients are calculated for two different substrate temperatures, 800 K and 1100 K. The heating of the substrate is realized by applying the Andersen heat bath to the system,^[25] followed by applying the Berendsen heat bath.^[26] Indeed, because of the perfect symmetry of the simulated crystal, the atoms of the constructed substrate all experience the same interatomic forces, causing in-phase vibrations. When heating the substrate immediately by applying the Berendsen heat bath, the Berendsen velocity rescaling amplifies the in-phase vibrations, resulting in high non-physical vibration amplitudes. Applying the Andersen heat bath first up to a substrate temperature of about 100 K, avoids this non-physical behavior: the stochastic Andersen heat bath disrupts the perfection of the vibrations of the atoms in the crystal. Subsequently, the Berendsen rescaling could be applied to reach the desired temperature of the substrate.

Moreover, since the energy barrier of the (2×1) reconstruction of the bulk-terminated diamond (111) surface is very low,^[22,24] heating the clean bulk-terminated diamond (111) substrate leads to reconstruction at the surface. It is known that hydrogen atoms stabilize the diamond (111) surface and prevent reconstruction.^[22,24] To reach the desired temperatures of the clean non-reconstructed (111) diamond substrates, the hydrogenated diamond (111) substrate is heated, followed by removal of the hydrogen atoms.

During the simulation of the impacts, no heat bath is applied. The simulated impacts of the considered particles are normal to the surface of the constructed substrates. The initial $\{x,y\}$ position of the particle is chosen randomly and at a distance above the substrate (z direction) beyond the outer cutoff radius of the interatomic potential. Periodic boundary conditions are enforced in the $\pm x$ - and $\pm y$ -directions. The initial translational, rotational, and vibrational energies correspond to a gas temperature of 2120 K above the substrate surface.^[9] Here, the common assumption is made that the translational, rotational, and vibrational modes of the hydrocarbon species are in equilibrium.^[1,27] Each impact is followed for 2 ps, using variable time steps between 10^{-6} and 10^{-4} ps. After each impact, any unbounded atoms are removed, as well as clusters not bonded to the substrate (i.e., clusters moving away from the substrate). The impacts of all the species listed above for a specified substrate temperature and geometry, are repeated 1000 times. Each impact is analyzed individually. The fraction of impacts resulting in a sticking or etch event yield the sticking and etch coefficients, respectively.

3. Results and Discussion

Since the clean diamond $(100)2 \times 1$ and $(111)1 \times 1$ surfaces contain no hydrogen atoms, and the kinetic energy of the impacting particles is as low as 0.274 eV, chemisorp-

tion ("sticking") and reflection of the impacting particles are the only processes occurring at the substrate surface. The sticking behavior of the investigated species on these surfaces are presented in Sections 3.1–3.5.

On the other hand, our simulations show that the only process occurring at the hydrogenated diamond $(100)2 \times 1$ and $(111)1 \times 1$ surfaces (represented by $(100)2 \times 1:2H$ and $(111)1 \times 1:H$, respectively; the suffixes indicate the number of adsorbate atoms within the complete unit cell),^[22] are hydrogen etching and reflection of the impacting particles. The etch behavior of the hydrocarbon species on the hydrogenated surfaces are discussed in Section 3.6.

3.1. Sticking Behavior of the CH_x Series

From Table 1, it can be seen that the total sticking coefficient for both diamond surfaces at both substrate temperatures decreases from C (sticking coefficient between 0.9 and 1) to CH_4 (sticking coefficient 0.0).

For hydrogen-poor plasmas, the carbon atom is predicted to be the CH_x species with the highest concentration above the substrate ($\sim 10^{12} \text{ cm}^{-3}$, other CH_x species, $\sim 10^{10}$ – 10^{11} cm^{-3}).^[9] Since the carbon atom is the most reactive CH_x species at both diamond surfaces at the lower substrate temperature, it seems to be the most important CH_x species for the growth of UNCD.

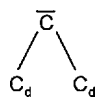
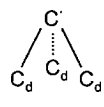
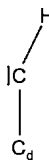
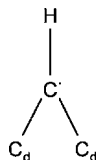
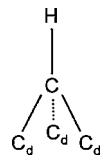
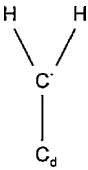
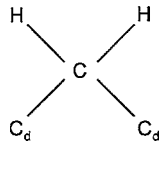
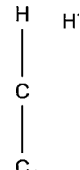
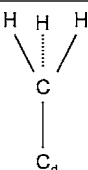
In contrast to that, CH_3 appears to be the CH_x species with the highest concentration above the substrate ($\sim 10^{13} \text{ cm}^{-3}$, other CH_x species, $\sim 10^7$ – 10^9 cm^{-3}) in a hydrogen-rich plasma created for the deposition of NCD.^[9] Although the sticking coefficient of CH_3 at both diamond surfaces is calculated to be as low as 0.11 for the increased substrate temperature, the CH_3 species is predicted to have the most sticking events of all CH_x species at typical deposition conditions of NCD.

The decreasing reactivity corresponds to a decreasing number of free electrons of the species from four (C) to zero (CH_4). Since the free electrons of the impacting particle can form bonds to the surface, the reactivity and thus the sticking efficiency of a species depends on the number of free electrons of that species.

Since the sticking efficiency does not decrease linearly, there must be a second effect influencing the total sticking coefficient. Indeed, CH and CH_3 have a higher and lower sticking coefficient, respectively, than expected for a linear decrease of the sticking coefficient. This non-linear decrease of the sticking can be attributed to sterical hindrance caused by hydrogen atoms bonded to the impacting carbon atoms. The more hydrogen atoms are bonded to the impacting carbon atoms, the more they are shielded from the surface, preventing sticking to the surface. This results in a lowered sticking efficiency.

The calculated sticking coefficients confirm the predictions made by Larsson et al.^[28] Based on ab initio calculations, the reactivity of CH_2 at a diamond (111) surface was predicted to be higher than the reactivity of CH_3 .

Table 1. Calculated sticking coefficients and corresponding errors of the CH_x species ($x=0-4$) on diamond (100) 2×1 and diamond (111) 1×1 surfaces at two different substrate temperatures. The errors are calculated as the unbiased estimates of the standard deviation corresponding to a binomial distribution. Two numbers are considered to be not significantly different if their error ranges overlap. Beside the total sticking coefficients, the various configurations of the stucked species and relative contribution to the total sticking coefficient (%) are given (configurations of stucked species with relative contribution of 5% or less for all four simulation conditions are not shown). One of the resonance contributors is shown, although others are possible.

		CH_x			
		C			
	T_{sub}	total sticking coefficient			
diamond (100) 2×1	800 K	0.98 ± 0.00	68.6%	22.8%	8.2%
	1100 K	0.97 ± 0.01	68.2%	22.5%	7.5%
diamond (111) 1×1	800 K	0.98 ± 0.00	61.1%	21.7%	16.1%
	1100 K	0.91 ± 0.01	52.8%	25.6%	20.8%
		CH			
	T_{sub}	total sticking coefficient			
diamond (100) 2×1	800 K	0.87 ± 0.01	70.9%	23.6%	5.1%
	1100 K	0.88 ± 0.01	66.3%	27.9%	5.2%
diamond (111) 1×1	800 K	0.86 ± 0.01	65.5%	24.8%	9.8%
	1100 K	0.83 ± 0.01	55.2%	31.3%	13.0%
		CH_2			
	T_{sub}	total sticking coefficient			
diamond (100) 2×1	800 K	0.53 ± 0.02	81.1%	10.3%	8.6%
	1100 K	0.55 ± 0.02	73.9%	13.3%	12.8%
diamond (111) 1×1	800 K	0.51 ± 0.02	82.1%	7.2%	7.6%
	1100 K	0.47 ± 0.02	85.1%	8.1%	3.6%
		CH_3			
	T_{sub}	total sticking coefficient			
diamond (100) 2×1	800 K	0.13 ± 0.01	81.1%		
	1100 K	0.11 ± 0.01	72.5%		
diamond (111) 1×1	800 K	0.11 ± 0.01	98.2%		
	1100 K	0.11 ± 0.01	91.5%		
		CH_4			
	T_{sub}	total sticking coefficient			
diamond (100) 2×1	800 K	0.00 ± 0.00			
	1100 K	0.00 ± 0.00			
diamond (111) 1×1	800 K	0.00 ± 0.00			
	1100 K	0.00 ± 0.00			

Furthermore, from Table 1, it can be seen that the substrate temperature alters the sticking efficiency on the diamond (100) 2×1 surface by, at most, 0.02 for CH_2 and CH_3 . In contrast to that, a higher substrate temperature significantly lowers the sticking efficiency on the diamond (111) 1×1 surface by 0.07, 0.03, and 0.04 for C, CH, and CH_2 , respectively. This different temperature effect can be attributed to the different structures of the substrate

surfaces. At the diamond (100) 2×1 surface, the atoms are arranged in dimer chains, whereas the surface atoms of the diamond (111) 1×1 surface are not bonded to each other (see Fig. 1).^[23,24] These structural differences result in a different temperature-dependence of the surface mobility of the atoms, as can be seen in Table 2; when the substrate temperature rises from 800 K to 1100 K, the average root mean square displacement of the surface atoms from their

Table 2. Calculated average root mean square displacement (\AA) of the surface atoms from their average $\{x,y\}$ position in 10^{-4} ps.

	800 K	1100 K	relative increase
diamond (100) 2×1	0.167	0.193	13.7%
diamond (111) 1×1	0.131	0.210	60.2%

average $\{x,y\}$ position at the diamond (100) 2×1 and (111) 1×1 surface increases by 13.7% and 60.2%, respectively. This significant gain of the $\{x,y\}$ mobility of the diamond (111) 1×1 surface atoms upon increase of the temperature induces an increase of the probability that within the simulation time a stucked species will desorb again. This lowers the overall sticking efficiency of the species at the diamond (111) 1×1 surface. As the mobility of the surface atoms at the diamond (100) 2×1 surface is less affected, the total sticking efficiency of most of the species is not affected significantly by the temperature.

Besides the total sticking coefficients of the species, the relative contributions of the most important configurations to the total sticking coefficient of every species are listed in Table 1. In general, it appears that it is more probable that a stucked species is bonded by one bond to the surface than by two or three bonds. For growth of diamond structures, the formation of tetrahedral structures, i.e., high coordinated adatoms, is required.

As can be seen from Table 1, at a higher substrate temperature, higher coordination numbers of stucked C and CH radicals on the diamond (111) 1×1 surface become significantly more probable. In contrast to that, a higher substrate temperature of the diamond (100) 2×1 surface has a less pronounced effect on the coordination of adatoms. The different influence of the substrate temperature on the adatom coordination can also be explained by the different gain of $\{x,y\}$ mobility of the surface atoms of diamond (100) 2×1 and (111) 1×1 . Since the surface atoms of the diamond (111) 1×1 surface experience a significant increase of their mobility, it becomes more probable that an impacting radical is close enough to more than one surface atom to form various single bonds. This effect results in higher adatom coordination. For the diamond (100) 2×1 surface, the substrate temperature increases the $\{x,y\}$ mobility by only 13.7%, and thus the adatom coordination does not experience a striking shift.

3.2. Sticking Behavior of the C_2H_x Series

Analogous to the observations made for the CH_x series, it is seen from Table 3 that as the number of free electrons decreases from two (C_2) to zero (C_2H_2), and from one to zero (C_2H_3 to C_2H_4 , and C_2H_5 to C_2H_6), the total sticking efficiency decreases as well. Moreover, for particles containing the same number of free electrons (e.g., C_2H_3 and C_2H_5), the sticking coefficient differs significantly. Indeed, the more hydrogen atoms the species contain, the more the carbon

atoms of the species are shielded from the surface (sterical hindrance), and thus the lower their total sticking coefficient. Hence, again, the sticking efficiency of the species seems to depend on their number of free electrons and hydrogen atoms.

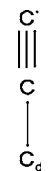
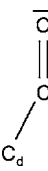
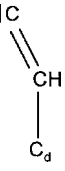
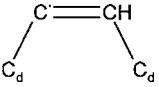
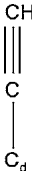
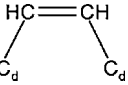
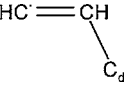
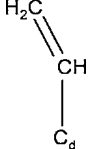
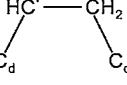
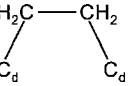
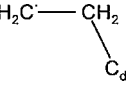
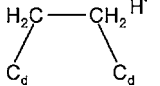
For typical deposition conditions of UNCD and NCD, the C_2H_2 species is calculated to be the C_2H_x species with the highest concentrations above the substrate ($\sim 10^{15} \text{ cm}^{-3}$ and $\sim 10^{14} \text{ cm}^{-3}$, other C_2H_x species: $\sim 10^5$ – 10^{12} cm^{-3} and $\sim 10^4$ – 10^{12} cm^{-3} , for the lower and higher substrate temperature, respectively).^[9] Although other C_2H_x species have higher sticking efficiencies than C_2H_2 (sticking coefficient of C_2H_2 , 0.1–0.4 and 0.1–0.3 for the lower and higher substrate temperature, respectively), the C_2H_2 species is predicted to have the most sticking events of all C_2H_x species at typical deposition conditions of UNCD and NCD. This is because of its high concentration above the substrate.

The results for the C_2H_x series again confirm the predictions made by Larsson et al.^[28] The reactivity of C_2H at a diamond (111) surface was predicted to be higher than the reactivity of C_2H_2 . The high reactivity of C_2 on diamond (100) was also predicted by ab initio and DFT calculations.^[13]

From Table 3, we can again conclude that the effect of the substrate temperature on the sticking efficiency on the diamond (111) 1×1 and (100) 2×1 surfaces is different. Except for C_2 and C_2H_6 , the sticking efficiency of the C_2H_x series on the diamond (111) 1×1 surface is lowered significantly by a higher substrate temperature, and the sticking coefficient on the diamond (100) 2×1 surface is not. As explained above, this results from the different temperature-induced gain of $\{x,y\}$ mobility of the diamond (100) 2×1 and (111) 1×1 surface atoms (see Table 2). Furthermore, a higher substrate temperature promotes a higher carbon coordination of the adatoms. For C_2 , at higher substrate temperatures, one-coordination of the carbon atom bonded to the surface becomes less probable, and two-coordination becomes more probable. Here, the effect is again more pronounced for the diamond (111) 1×1 surface than for the diamond (100) 2×1 surface. Indeed, the probability of a one-coordinated carbon adatom decreases for the diamond (100) 2×1 and (111) 1×1 surfaces by 9.4% and 12.6%, respectively. The probability of a two-coordinated adatom increases by 8.4% and 11.7% for the diamond (100) 2×1 and (111) 1×1 surfaces, respectively. This is in agreement with the different gain of $\{x,y\}$ mobility of the diamond (100) 2×1 and (111) 1×1 surface atoms (see above).

For the species C_2H , C_2H_2 , C_2H_3 , and C_2H_4 , the relative probability that both carbon atoms of a stucked species form bonds to the diamond (111) 1×1 surface increases at higher temperatures. The same observations are made for C_2H , C_2H_3 , and C_2H_4 on the diamond (100) 2×1 surface. Thus, at higher temperatures, the distribution of the adatom coordination shifts to higher coordination. This can be explained as follows; a species initially bonded by one carbon atom to the surface will be, at higher temperature, more capable of evolving into a configuration in which the

Table 3. Calculated sticking coefficients and corresponding errors of the C_2H_x species ($x=0-6$) on diamond (100) 2×1 and diamond (111) 1×1 surfaces at two different substrate temperatures. The errors are calculated as the unbiased estimates of the standard deviation corresponding to a binomial distribution. Beside the total sticking coefficients, the various configurations of the stuck species and relative contribution to the total sticking coefficient (%) are given (configurations of stuck species with relative contribution of 5% or less for all four simulation conditions are not shown). One of the resonance contributors is shown, although others are possible.

		C_2H_x			
		C_2			
	T_{sub}	total sticking coefficient			
diamond (100) 2×1	800 K	1.00 ± 0.00	56.4%	40.8%	
	1100 K	1.00 ± 0.00	47.0%	49.2%	
diamond (111) 1×1	800 K	1.00 ± 0.00	81.3%	16.4%	
	1100 K	1.00 ± 0.00	68.7%	28.1%	
		C_2H			
	T_{sub}	total sticking coefficient			
diamond (100) 2×1	800 K	0.86 ± 0.01	79.1%	11.4%	5.8%
	1100 K	0.85 ± 0.01	75.9%	13.0%	4.5%
diamond (111) 1×1	800 K	0.94 ± 0.01	66.3%	15.7%	13.9%
	1100 K	0.87 ± 0.01	66.3%	17.1%	10.8%
		C_2H_2			
	T_{sub}	total sticking coefficient			
diamond (100) 2×1	800 K	0.10 ± 0.01	34.7%	35.6%	
	1100 K	0.11 ± 0.01	28.6%	31.4%	
diamond (111) 1×1	800 K	0.39 ± 0.02	46.2%	52.6%	
	1100 K	0.30 ± 0.01	73.8%	24.2%	
		C_2H_3			
	T_{sub}	total sticking coefficient			
diamond (100) 2×1	800 K	0.45 ± 0.02	66.8%	17.3%	
	1100 K	0.43 ± 0.02	59.2%	20.0%	
diamond (111) 1×1	800 K	0.47 ± 0.02	57.7%	33.9%	
	1100 K	0.41 ± 0.02	54.0%	34.5%	
		C_2H_4			
	T_{sub}	total sticking coefficient			
diamond (100) 2×1	800 K	0.07 ± 0.01	37.7%	46.4%	
	1100 K	0.08 ± 0.01	43.6%	43.6%	
diamond (111) 1×1	800 K	0.19 ± 0.01	63.1%	31.6%	
	1100 K	0.15 ± 0.01	67.5%	22.5%	
		C_2H_5			
	T_{sub}	total sticking coefficient			
diamond (100) 2×1	800 K	0.06 ± 0.01	68.3%		
	1100 K	0.05 ± 0.01	67.3%		
diamond (111) 1×1	800 K	0.09 ± 0.01	77.8%		
	1100 K	0.07 ± 0.01	57.1%		

C_2H_x		
	T_{sub}	C_2H_6 total sticking coefficient
diamond (100)2 × 1	800 K	0.00 ± 0.00
	1100 K	0.00 ± 0.00
diamond (111)1 × 1	800 K	0.00 ± 0.00
	1100 K	0.00 ± 0.00

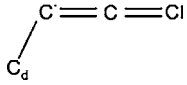
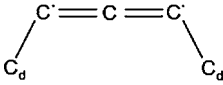
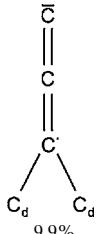
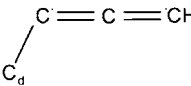
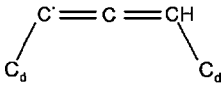
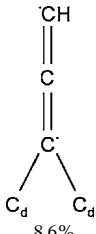
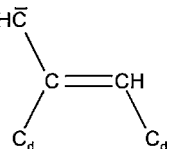
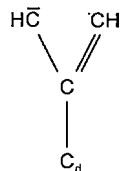
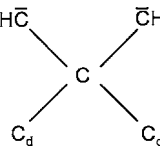
formation of a second bond by the second carbon atom is possible.

3.3. Sticking Behavior of the C_3H_x Series

For the C_3H_x series, we can again conclude that the number of free electrons and hydrogen atoms determines the reactivity of the species (see Table 4).

C_3 is predicted to be the C_3H_x species with the highest concentration above the substrate ($\sim 10^{14} \text{ cm}^{-3}$, other C_3H_x species: $\sim 10^{11} - 10^{13} \text{ cm}^{-3}$) under typical conditions applied for the deposition of UNCD.^[9] Since C_3 has the highest sticking coefficient at the lower substrate temperature (almost 1 for the diamond (100)2 × 1 and (111)1 × 1 surfaces), it appears to be the most important C_3H_x species for the growth of UNCD. For typical conditions applied for

Table 4. Calculated sticking coefficients and corresponding errors of the C_3H_x species ($x=0-2$) on diamond (100)2 × 1 and diamond (111)1 × 1 surfaces at two different substrate temperatures. The errors are calculated as the unbiased estimates of the standard deviation corresponding to a binomial distribution. Beside the total sticking coefficients, the various configurations of the stucked species and relative contribution to the total sticking coefficient (%) are given (configurations of stucked species with relative contribution of 5% or less for all four simulation conditions are not shown). One of the resonance contributors is shown, although others are possible.

C_3H_x						
	T_{sub}	C_3 total sticking coefficient				
diamond (100)2 × 1	800 K	0.96 ± 0.01	46.8%	29.6%	9.9%	
	1100 K	0.96 ± 0.01	37.3%	33.9%	9.8%	
diamond (111)1 × 1	800 K	0.99 ± 0.00	61.5%	13.5%	6.6%	
	1100 K	0.96 ± 0.01	56.0%	16.5%	8.3%	
	T_{sub}	C_3H total sticking coefficient				
diamond (100)2 × 1	800 K	0.84 ± 0.01	50.1%	20.5%	8.6%	
	1100 K	0.86 ± 0.01	44.1%	21.4%	10.4%	
diamond (111)1 × 1	800 K	0.95 ± 0.01	42.2%	12.6%	5.3%	
	1100 K	0.88 ± 0.01	36.9%	15.9%	6.8%	
	T_{sub}	C_3H_2 total sticking coefficient				
diamond (100)2 × 1	800 K	0.69 ± 0.01	30.4%	27.5%	10.1%	
	1100 K	0.71 ± 0.01	28.2%	25.4%	9.9%	
diamond (111)1 × 1	800 K	0.77 ± 0.01	29.5%	21.1%	5.7%	
	1100 K	0.70 ± 0.01	25.0%	18.2%	7.8%	

the deposition of NCD, C_3H_2 was found to be the C_3H_x species with the highest concentration ($\sim 10^{12} \text{ cm}^{-3}$, other C_3H_x species, $\sim 10^8 \text{ cm}^{-3}$).^[9] Since the sticking coefficient of C_3H_2 at both diamond surfaces is calculated to be 0.7 at high substrate temperature, the C_3H_2 species is predicted to have the most sticking events of all C_3H_x species at typical deposition conditions of NCD.

The increased substrate temperature has no (C_3) or only a weak effect in increasing the sticking efficiency on the diamond $(100)2 \times 1$ surface. Since the sticking efficiency of C_3H and C_3H_2 on the diamond $(100)2 \times 1$ surface is increased by only 0.02, the underlying effect of the enhanced sticking efficiency is too weak to identify. The sticking efficiency of all C_3H_x species on the diamond $(111)1 \times 1$ surface, however, decreases significantly as the substrate temperature increases, which is consistent with the results presented above.

On the other hand, the increased substrate temperature again promotes higher coordination of the adatoms; for C_3 and C_3H , the formation of two bonds by the outer two carbon atoms to the diamond $(100)2 \times 1$ and $(111)1 \times 1$ surface becomes more probable at higher temperatures. Furthermore, at higher temperatures, it becomes slightly more probable that one carbon atom of C_3 , C_3H , and C_3H_2 forms two bonds to the diamond $(111)1 \times 1$ surface, and one carbon atom of C_3H forms two bonds to the diamond $(100)2 \times 1$ surface. These results are in agreement with the results for the C_2H_x series.

In contrast to the results obtained for the C_2H_x series, it becomes less probable that two adjacent carbon atoms of C_3H_2 both form one bond to the surface when increasing the temperature.

3.4. Sticking Behavior of the C_4H_x Series

As we concluded for the other series, the sticking efficiency of the C_4H_x species depends again on their number of free electrons and hydrogen atoms (see Table 5).

For typical deposition conditions of UNCD and NCD, C_4H_2 was calculated to be the C_4H_x species with the highest concentration above the substrate ($\sim 10^{13} \text{ cm}^{-3}$ and $\sim 10^{10} \text{ cm}^{-3}$ for UNCD and NCD, respectively, other C_4H_x species, $\sim 10^{10}$ – 10^{11} cm^{-3} and $\sim 10^1$ – 10^5 cm^{-3} for UNCD and NCD, respectively).^[9] Since the sticking coefficient of C_4H_2 is fairly high (0.5–0.9 and 0.5–0.8 at lower and higher substrate temperatures, respectively), it is predicted to have the most sticking events of all C_4H_x species at typical deposition conditions of UNCD and NCD.

A higher substrate temperature again lowers significantly the sticking efficiency of all C_4H_x species on the diamond $(111)1 \times 1$ surface. This effect results, as explained above, from the increased $\{x,y\}$ mobility of the diamond $(111)1 \times 1$ surface atoms. For the diamond $(100)2 \times 1$ surface, the substrate temperature only significantly affects the sticking efficiency of C_4H . Since the sticking coefficient of C_4H

increases by only 0.02, the underlying effect that increases the sticking efficiency at higher temperatures, is probably weak.

For the C_4H_x series, a higher substrate temperature influences the adatom coordination less than we would expect. C_4H_2 is the only species for which the increased substrate temperature shifts the relative distribution of the adatom coordination to higher adatom coordinations. Indeed, the formation of one bond to the surface becomes less probable, and the formation of two bonds by adjacent carbon atoms becomes more probable. In contrast to the results presented above, the effect is more pronounced for the diamond $(100)2 \times 1$ surface than for the diamond $(111)1 \times 1$ surface.

3.5. Sticking Behavior of H and H_2

Although the hydrogen atom is much smaller than the other investigated species, it has a relatively high sticking efficiency on both diamond surfaces (see Table 6). As the substrate temperature increases, the sticking efficiency decreases significantly for both surfaces, which is in agreement with the results for the other species.

For the diamond $(100)2 \times 1$ surface, the sticking efficiency decreases less strongly than for the diamond $(111)1 \times 1$ surface. This can again be attributed to the different gain in $\{x,y\}$ mobility of the diamond $(100)2 \times 1$ and $(111)1 \times 1$ surface atoms (see above).

The sticking efficiency of H_2 is calculated to be lower than 0.05 on both diamond surfaces and at both substrate temperatures. The lower reactivity of molecular hydrogen compared to atomic hydrogen, is in agreement with quantum mechanical calculations by Zhan et al.^[29] The energy difference between the highest occupied molecular orbital (HOMO) of a hydrogen species and the lowest unoccupied molecular orbital (LUMO) of sp^3 -bonded carbon is lower for H than for H_2 .^[29] Therefore, Zhang et al. predict a higher reactivity for H with sp^3 -bonded carbon than for H_2 , which is also reflected in our calculations.

The high sticking coefficient of atomic hydrogen is in agreement with the assumption that the diamond surface is nearly fully saturated with hydrogen.^[17] This hydrogen termination of the surface is required for the growth of metastable diamond, since atomic hydrogen is thought to stabilize the sp^3 diamond lattice, preventing the reconstruction of the surface to graphite.^[17,30]

3.6. Etch Behavior on Hydrogenated Diamond Surfaces

As mentioned above, during diamond CVD growth, the diamond surfaces are hydrogen-terminated. Hence, these hydrogen atoms at the diamond surface need to be removed to create reactive sites for carbon-containing species.^[17] Therefore, the etch behavior of the hydrocarbon species on the hydrogenated surfaces is investigated.

Our calculations predict that the only species that etches hydrogen from the hydrogenated diamond surfaces with a

Table 5. Calculated sticking coefficients and corresponding errors of the C_4H_x ($x=0-2$) species on diamond $(100)2 \times 1$ and diamond $(111)1 \times 1$ surfaces at two different substrate temperatures. The errors are calculated as the unbiased estimates of the standard deviation corresponding to a binomial distribution. Beside the total sticking coefficients, the various configurations of the stucked species and relative contribution to the total sticking coefficient (%) are given (configurations of stucked species with relative contribution of 5% or less for all four simulation conditions are not shown). One of the resonance contributors is shown, although others are possible.

		C_4H_x				
		C_4	C_4H		C_4H_2	
T_{sub}	total sticking coefficient					
diamond $(100)2 \times 1$	800 K	0.97 ± 0.01	47.6%			
	1100 K	0.96 ± 0.01	45.4%			
diamond $(111)1 \times 1$	800 K	0.99 ± 0.00	52.4%			
	1100 K	0.97 ± 0.01	49.1%			
diamond $(100)2 \times 1$	800 K	0.84 ± 0.01	48.8%	34.5%	8.3%	
	1100 K	0.86 ± 0.01	45.3%	33.7%	9.3%	
diamond $(111)1 \times 1$	800 K	0.97 ± 0.01	39.2%	11.3%	10.3%	
	1100 K	0.90 ± 0.01	36.7%	8.9%	8.9%	
diamond $(100)2 \times 1$	800 K	0.49 ± 0.02	55.1%	16.3%	10.2%	
	1100 K	0.52 ± 0.02	44.2%	25.0%	7.7%	
diamond $(111)1 \times 1$	800 K	0.87 ± 0.02	32.2%	33.3%	6.9%	
	1100 K	0.76 ± 0.02	28.9%	35.5%	5.3%	

probability of 0.05 or higher, is C_2 . As can be seen from Table 7, the etch coefficients are higher for the hydrogenated diamond $(111)1 \times 1$ surface than for the hydrogenated diamond $(100)2 \times 1$ surface. This can be explained by the different bonding structure of the diamond surfaces;

Table 6. Calculated sticking coefficients and corresponding errors of H on diamond $(100)2 \times 1$ and $(111)1 \times 1$ surfaces. The errors are calculated as the unbiased estimates of the standard deviation corresponding to a binomial distribution.

	T_{sub}	sticking coefficient
diamond $(100)2 \times 1$	800 K	0.79 ± 0.02
	1100 K	0.75 ± 0.02
diamond $(111)1 \times 1$	800 K	0.85 ± 0.02
	1100 K	0.75 ± 0.02

the hydrogen atoms at the diamond $(100)2 \times 1:2H$ surface are bonded to carbon atoms which are arranged in dimer chains, and they are localized close to the dimer chains. This results in distinctive surface areas with high and low amounts

Table 7. Calculated probabilities and corresponding errors of C_2 etching one hydrogen atom from a hydrogenated diamond $(100)2 \times 1$ and $(111)1 \times 1$ surfaces (diamond $(100)2 \times 1:2H$ and diamond $(111)1 \times 1:H$). The probability of more than one etched hydrogen atom per C_2 impact is negligible. The errors are calculated as the unbiased estimates of the standard deviation corresponding to a binomial distribution.

	T_{sub}	etch coefficient
diamond $(100)2 \times 1:2H$	800 K	0.43 ± 0.02
	1100 K	0.50 ± 0.02
diamond $(111)1 \times 1:H$	800 K	0.81 ± 0.02
	1100 K	0.87 ± 0.02

of hydrogen. In contrast to that, the hydrogen atoms at the diamond (111) 1×1 :H surface are more homogeneously distributed. The probability that an impacting carbon dimer will be close enough to a hydrogen atom to form a bond with it, is thus higher at the diamond (111) 1×1 :H surface. As the substrate temperature increases, the bond breaking between a diamond carbon atom and a hydrogen atom will be facilitated. Indeed, the etch efficiency increases at higher substrate temperatures.

In the past, investigations were carried out to unravel the role of C_2 in (ultra)nanocrystalline diamond growth. As mentioned above, Gruen et al. found that C_2 is a very reactive species at the diamond (100) surface, suggesting that it is a possible growth species of UNCD.^[13] On the other hand, Rabeau et al. showed that NCD growth is independent of the presence of C_2 .^[16]

The concentration of C_2 above the substrate under typical UNCD deposition conditions is calculated to be in the order of 10^{11} cm^{-3} ,^[9] and our MD simulations predict that it is the only species with a significant etching coefficient (>0.05). Therefore, this suggests that C_2 is the most important species for the creation of reactive sites, and hence probably also for UNCD growth.

In contrast to that, the concentration of C_2 above the substrate under typical NCD deposition conditions is found to be in the order of only 10^6 cm^{-3} .^[9] Therefore, C_2 cannot be the most important etching species at typical deposition conditions of NCD. Although our calculations predict a very low etch coefficient of the hydrogen atom at high temperature (about 0.04), the high ratio of hydrogen atom concentration to hydrocarbon concentration above the substrate (27.8 for NCD growth) implicates that hydrogen atoms are probably the most important etching species for NCD growth.^[9] This is in agreement with the fact that NCD growth appears to be independent of C_2 .^[16]

3.7. Implications for (U)NCD Growth

From the results presented above, we conclude that a higher substrate temperature promotes higher adatom coordination, which is required for the growth of diamond structures. This temperature-induced effect on the adatom coordination might explain why larger diamond crystals, as typical for NCD, can be grown at higher temperatures, and why UNCD, with its high percentage of disordered phases (up to 10%),^[31] can be grown at lower substrate temperatures than NCD.

Furthermore, the substrate temperature influences the sticking behavior of the species on a diamond (100) 2×1 and (111) 1×1 surface differently. For the diamond (111) 1×1 surface, although the total sticking coefficients of the species are lowered by a higher substrate temperature, an increased substrate temperature shifts the distribution of adatom coordination on the diamond (111) 1×1 surface to higher

coordinations. These effects are less pronounced for the diamond (100) 2×1 surface. Therefore, we conclude that diamond (111) growth is promoted by a higher temperature to a greater extent than diamond (100) growth. Therefore, the experimental ratio of the diamond (111) and (100) growth has to increase at higher temperatures. An increase of the ratio of diamond (111) and (100) growth when the substrate temperature is raised from 800 K to 1100 K, is in agreement with earlier experimental measurements by Maeda et al.^[32]

4. Conclusions

In this study, we investigated the reaction behavior of various hydrocarbon species on clean and hydrogenated diamond (100) 2×1 and (111) 1×1 surfaces by means of classical molecular dynamics simulations. At the clean diamond surfaces, chemisorption ("sticking") and reflection of the impacting species were the only observed processes. In contrast, hydrogen etching and reflection were the only processes occurring at the hydrogenated diamond surfaces.

Our calculations of the sticking behavior and earlier studies of the concentration of the hydrocarbon species in the plasma implicate that of their series, C, C_2H_2 , C_3 , and C_4H_2 are the most important growth species for UNCD growth.^[9] For NCD growth, CH_3 , C_2H_2 , C_3H_2 , and C_4H_2 appear to be the most important growth species.

The sticking efficiency of the investigated hydrocarbon species decreases significantly, as the number of free electrons decreases and the number of hydrogen atoms of the species increases. The effect of an increased substrate temperature differs for the diamond (100) 2×1 and (111) 1×1 surfaces, which can be attributed to a difference of surface bonding structure and hence surface atoms mobilities. These results have implications on the effect of the temperature on the experimental ratio of diamond (100) and (111) growth, which are indeed confirmed by earlier experimental investigations.^[32]

Finally, our calculations predict that C_2 is the only significant etching species at hydrogenated diamond surfaces. The etching coefficient increases at higher substrate temperature. Indeed, at higher temperatures, the bond breaking of the carbon and hydrogen surface atoms is facilitated. Our calculations of the etching coefficient in combination with earlier studies implicate that C_2 is the most important etching species of UNCD, but not of NCD.^[9] This is in agreement with the fact that NCD growth appears to be independent of C_2 .^[16]

Received: November 5, 2007

Revised: February 22, 2008

[1] D. M. Gruen, *Annu. Rev. Mater. Sci.* **1999**, 29, 211.

[2] J. Philip, P. Hess, T. Feygelson, J. E. Butler, S. Chattopadhyay, K. H. Chen, L. C. Chen, *J. Appl. Phys.* **2003**, 93, 2164.

- [3] V. S. Purohit, D. Jain, V. G. Sathe, V. Ganesan, S. V. Bhoraskar, *J. Phys. D: Appl. Phys.* **2007**, *40*, 1794.
- [4] M. D. Fries, Y. K. Vohra, *Diamond Relat. Mater.* **2004**, *13*, 1740.
- [5] C. Zuiker, A. R. Krauss, D. M. Gruen, X. Pan, J. C. Li, R. Csencsits, A. Erdemir, C. Bindal, G. Fenske, *Thin Solid Films* **1995**, *270*, 154.
- [6] W. Okrój, M. Kamińska, L. Klimek, W. Szymański, B. Walkowiak, *Diamond Relat. Mater.* **2006**, *15*, 1535.
- [7] O. A. Williams, M. Nesládek, *Phys. Status Solidi A* **2006**, *203*, 3375.
- [8] A. R. Krauss, O. Auciello, D. M. Gruen, A. Jayatissa, A. Sumant, J. Tucek, D. C. Mancini, N. Moldovan, A. Erdemir, D. Ersoy, M. N. Gardos, H. G. Busmann, E. M. Meyer, M. Q. Ding, *Diamond Relat. Mater.* **2001**, *10*, 1952.
- [9] P. W. May, J. N. Harvey, J. A. Smith, Yu, A. Mankelevich, *J. Appl. Phys.* **2006**, *99*, 104907.
- [10] O. A. Williams, M. Daenen, J. D'Haen, K. Haenen, J. Maes, V. V. Moshchalkov, M. Nesládek, D. M. Gruen, *Diamond Relat. Mater.* **2006**, *15*, 654.
- [11] Z. L. Wang, J. J. Li, Z. H. Sun, Y. L. Li, Q. Luo, C. Z. Gu, Z. Cui, *Appl. Phys. Lett.* **2007**, *90*, 133118.
- [12] A. Erdemir, C. Bindal, G. R. Fenske, C. Zuiker, A. R. Krauss, D. M. Gruen, *Diamond Relat. Mater.* **1996**, *5*, 923.
- [13] D. M. Gruen, P. C. Redfern, D. A. Horner, P. Zapol, L. A. Curtiss, *J. Phys. Chem. B* **1999**, *103*, 5459.
- [14] G. Lombardi, K. Hassouni, F. Bénédic, F. Mohasseb, J. Röpcke, A. Gicquel, *J. Appl. Phys.* **2004**, *96*, 6739.
- [15] K. Teii, T. Ikeda, *Appl. Phys. Lett.* **2007**, *90*, 111504.
- [16] J. R. Rabeau, P. John, J. I. B. Wilson, Y. Fan, *J. Appl. Phys.* **2004**, *96*, 6724.
- [17] P. W. May, *Phil. Trans. Roy. Soc. Lond. A* **2000**, *358*, 473.
- [18] J. Tanaka, C. F. Abrams, D. B. Graves, *J. Vac. Sci. Technol. A* **2000**, *18*, 938.
- [19] D. W. Brenner, *Phys. Rev. B* **1990**, *42*, 9458.
- [20] A. J. Dyson, P. V. Smith, *Surf. Sci.* **1994**, *316*, 309.
- [21] W. C. Swope, H. C. Andersen, P. H. Berens, K. R. Wilson, *J. Chem. Phys.* **1982**, *76*, 637.
- [22] J. Ristein, *Appl. Phys. A* **2006**, *82*, 377.
- [23] T. Frauenheim, U. Stephan, P. Blaudeck, D. Porezag, H.-G. Busmann, W. Zimmermann-Edling, S. Lauer, *Phys. Rev. B* **1993**, *48*, 18189.
- [24] G. Kern, J. Hafner, G. Kresse, *Surf. Sci.* **1996**, *366*, 445.
- [25] H. C. Andersen, *J. Chem. Phys.* **1980**, *72*, 2384.
- [26] H. J. C. Berendsen, J. P. M. Postma, W. F. van Gunsteren, A. DiNola, J. R. Haak, *J. Chem. Phys.* **1984**, *81*, 3684.
- [27] G. Lombardi, F. Bénédic, F. Mohasseb, K. Hassouni, A. Gicquel, *Plasma Sources Sci. Technol.* **2004**, *13*, 375.
- [28] K. Larsson, J.-O. Carlsson, S. Lunell, *Phys. Rev. B* **1995**, *51*, 10003.
- [29] R. Zhang, T. Chu, C.-S. Lee, S.-T. Lee, *Chem. Vap. Deposition* **2000**, *6*, 227.
- [30] J. C. Angus, C. C. Hayman, *Science* **1988**, *214*, 913.
- [31] P. Zapol, M. Sternberg, L. A. Curtiss, T. Frauenheim, D. M. Gruen, *Phys. Rev. B* **2001**, *65*, 045403.
- [32] H. Maeda, K. Ohtsubo, M. Irie, N. Ohya, K. Kusakabe, S. Morooka, *J. Mater. Res.* **1995**, *10*, 3115.